JOURNAL OF Applied Polymer SCIENCE

Peering into Polypyrrole–SDS Nanodispersions: Rheological View

Rupali Gangopadhyay
Centre for Advanced Materials, Indian Association for the Cultivation of Science, Kolkata 32, West Bengal, India
Correspondence to: R. Gangopadhyay (E-mail: camrg@iacs.res.in)

ABSTRACT: Synthesis and rheological properties of a series of polypyrrole (PPy) nanodispersions stabilized by sodium dodecyl sulfate (SDS) are described here. Changes in particle size, morphology, spectroscopy (UV–vis), and rheological properties (steady and dynamic) of the dispersions with variation in PPy fraction were studied. PPy nanoparticles (20–50 nm) incorporated within large micellar entanglements (>700 nm) were identified from transmission electron micrograph and dynamic light scattering studies. On standing the dispersions, electrostatic interaction among the micelles via Fe^{3+} comes into play and the dispersion is gradually crosslinked to form a soft gel. Shear thinning generally observed for steady rheology measurements (1–500 s^{-1}) on freshly prepared dispersion is accounted for the breakdown of larger entanglements under high shear. The aged dispersion (before gelling), however, exhibits a viscosity plateau, characteristic of the crosslinked systems. The dispersion [with loss (G'') moduli > storage (G') moduli] behaves like a viscous liquid and resembles to semidilute polymeric solutions. Zimm model is roughly followed by the system as revealed from the respective slopes of G' and G'' curves. The partially crosslinked system (aged by 7 days) partly follows Maxwell model, and a crossover of G' and G'' corresponding to a single relaxation time is obtained. Stability of the dispersion, nanoscopic particle size, moderate conductivity, and shear thinning behavior encourage its prospect as conducting ink/paint. © 2012 Wiley Periodicals, Inc. J. Appl. Polym. Sci. 000: 000–000, 2012

KEYWORDS: polypyrrole; nanodispersion; SDS; rheology; modulus; viscosity

Received 2 April 2012; accepted 18 June 2012; published online
DOI: 10.1002/app.38218

INTRODUCTION

Study of rheology was originally proposed to describe and explain the flow and deformation of matter.[1,2] At present, it is a well-established tool for monitoring structural transitions and molecular interactions in solutions, blends, dispersions, emulsions, gels, etc. consisting of a large variety of materials including polymers, surfactants, and biomolecules. Understanding rheology of a liquid is highly important not only for fundamental interest but also for its applications as paint, coating, or edible items. Inherently conducting polymers (ICPs) having good color and electrical conductivity should have extensive use as conducting paint/printing ink. However, insoluble and infusible nature of these polymers has kept them away from formation of solution/melt and has seriously obstructed their rheological characterization as well as their manifold application in sophisticated devices.

So far, there have been a lot of efforts to overcome the intractability of ICP and to bring them into a stable solution/dispersion, using a soluble support polymer[3,4] or inorganic nanoparticles/colloid.[5] In a parallel stream of work, some long-chain sulfonate molecules such as dodecylbenzene sulfonic acid (DBSA) and camphor sulfonic acid were incorporated into the chains of polyaniline[6] and polypyrrole (PPy)[7] to improve their solubility in nonaqueous solvents. Very recently, the familiar anionic surfactants, viz., sodium dodecyl sulfate (SDS) and DBSA,[8] were also used to prepare stable dispersion of PAn and PPy in aqueous medium. In some cases, a nonionic surfactant and even a reverse microemulsion have also been exploited as effective medium for PAn stabilization.[9] Shape control of conducting polymer nanostructures is also possible using soft templates like micelle or reverse micelle.[10]

Stable solution or dispersion always has several advantages; it can be used for coating, film casting, and even printing in desired forms, if the stability and viscosity are optimized. Stabilization of PPy in aqueous/nonaqueous dispersion is therefore a popular approach toward improving processability of PPy. Printable conducting polymer formulations are supposed to have vast applications in printed devices, e.g., flexible batteries, light-emitting displays, microelectromechanical systems, and smart sensors. However, to understand the applicability of the dispersion as printing ink, rheological studies are highly important. To be precise, viscosity of the dispersion should be high

Additional Supporting Information may be found in the online version of this article.

enough to be held in the printer nozzle (without dripping) and low enough to allow spreading over the substrate (during printing). Under printing condition, the ink is under high shear rate within the nozzle; therefore, its behavior during shear (shear thinning/thickening) must be known from rheological studies. However, despite all successful attempts to improve solution processability of ICP, only few references regarding detailed rheological characterization of conducting polymer-based dispersions are available. Recently, Garai and Nandi[11] have explored the effect of Na-MMT clay loading on rheological properties of PAn-based gel nanocomposites in *m*-cresol. By increasing the clay fraction in composite the storage modulus was increased dramatically and gel melting temperature was also shifted to higher. We have studied steady and dynamic mechanical properties of a series of PAn-based dispersions in which a water-soluble polymer poly vinyl pyrrolidone (PVP)[12] and two anionic surfactants (SDS and DBSA)[13] were used as stabilizers to the PAn chain. In the PVP–PAn system,[12] hydrogen bonding between the polymers was established, and depending upon the fraction of PAn loading and extent of hydrogen bonding a sol-to-gel transition was observed. Just the reverse of this, i.e., a gel-to-sol transition was identified for PAn–DBSA system[13]; rheological studies have revealed this system as a flocculated one. On the other hand, PAn–SDS is a stabilized dispersion that behaves like an entangled polymer solution that never shows gel-like behavior. Yang et al.[14] have reported rheological properties of 2-acrylamido-2-methyl propanesulphonic acid (AMPS)-doped PAn dispersion in dichloroacetic acid; however, they have explored the effect of steady shear on viscosity at different conditions.

This article deals with steady and dynamic viscoelastic characterization of stable aqueous dispersion of PPy in the presence of a surfactant (SDS). There have been exhaustive studies on rheological properties of micellar solutions (mainly cationic) in the presence of salts.[15,16] PPy–SDS dispersion, on the other hand, presents a different system where an insoluble polymer is dispersed/stabilized by a surfactant and in this respect this system is also different from polymeric solutions or blends. We have concentrated our interest on studying the morphological and rheological characteristics of the system and have tried to explore its physical properties.

EXPERIMENTAL

Synthesis

Measured volume (0.6–1.0 mL) of pyrrole (Wako, Hokkaido, Japan) was added to the SDS solution (in water) of predetermined concentration (0.2–0.3*M*) on constant stirring at 20°C. After 1 h, $FeCl_3$ solution (maintaining pyrrole : $FeCl_3$ mole ratio 1 : 1.25) was added slowly to the pyrrole–SDS solution on constant sonication. Pyrrole starts to polymerize and highly viscous black-
colored solution/dispersion is obtained. The PPy–SDS dispersion is strongly adhered to glass or metal surfaces, but the films prepared from this are too brittle to handle freely.

Transmission Electron Micrograph

A total of 0.1 mL of PPy–SDS solution was diluted 20 times using SDS solution of same concentration (to prevent the precipitation on dilution) and sonicated well. One drop of the diluted solution was taken on a carbon-coated copper grid, and the image was taken at 200 kV using JEOL-JEM, 2010 Electron Microscope.

Dynamic Light Scattering

PPy–SDS dispersion, diluted 20-fold with 0.2*M* SDS solution, was subjected to dynamic light scattering (DLS) studies using Brookhaven Instruments (Model no. BI 200SM—Goniometer).

UV–Visible Absorption Spectroscopy

PPy–SDS dispersions were diluted with 0.2*M* SDS solution and were subjected to UV–vis spectroscopic measurements using Shimadzu UV 2550 Spectrophotometer.

Rheology

Steady and dynamic rheology measurements were performed on Rheometric Scientific Advanced Rheometric Expansion System (902-30004) (interfaced with a computer), using couette geometry. The cup diameter, bob diameter, and length are 34, 32, and 33 mm, respectively. Approximately 12 mL solution was required for each measurement, and after loading the solution into the cup the bob was lowered down to a fixed level so that the solution touches the upper edge of cup, makes a meniscus between two walls, and does not flow out. The solution-loaded couette was allowed to stand for 10 min to ensure the full relaxation of the sample and to get the temperature of the bath. Steady measurements were done under varying shear rate ranging from 0.1 to 500 s^{-1}, and dynamic measurements were done under angular frequency range from 0.1 to 100 $rads^{-1}$. Storage modulus (G'), loss modulus (G''), and few other relevant factors were studied. The effect of variation of strain amplitude from 1 to 500% was also monitored, and in some cases the solution was subjected to a steady preshearing for few minutes (up to 15 min) before starting the dynamic measurements. However, after each measurement, the solution was allowed to relax fully for at least 10 min before the next measurement to start. A circulating bath around the cup was used to fix the temperature at 25°C during measurements; temperature dependence of G', G'', etc. was also studied by varying the temperature from 10 to 50°C using the same solvent bath surrounding the cup fitted with a temperature controller.

RESULTS

General Aspects of the System

In this work, PPy has been synthesized in the presence of a surfactant that prevents the macroscopic precipitation of the polymer and keeps the insoluble polymer in dispersion. For its high molecular weight and sufficient solution viscosity, SDS was selected as the stabilizer for present purpose. The synthesis technique is similar to the standard chemical polymerization of pyrrole with two exceptions to be mentioned here. Lower synthesis temperature is always favorable to conducting polymers, but considering the Krafft temperature of SDS (16°C) the synthesis in the present case was performed at 20°C. Optimum pyrrole : $FeCl_3$ mole ratio for pyrrole polymerization is 1 : 2.25, but in the present case high-concentration multivalent Fe^{3+} ions cause the negatively charged SDS micelles to be agglomerated. At the same time, the rate of polymerization of pyrrole also becomes very high that is harmful to stability of the system. Considering

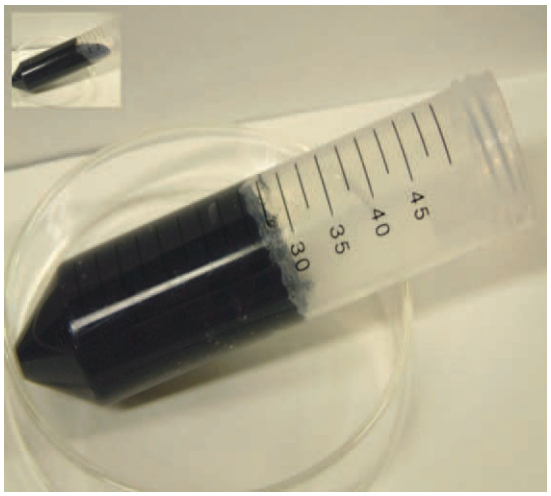

Figure 1. PPy–SDS colloidal dispersion transformed to gel after 30 days (freshly prepared dispersion shown in inset).

all these factors, an optimum mole ratio was fixed at 1 : 1.25. The PPy–SDS sample synthesized in the form of black viscous solution is stable up to 10 days (Figure 1 inset), after which the solution is gradually transformed to a very soft gel-like state. Primarily, this gel state is reversible and on gentle heating and stirring the sol state could be brought back. After substantial aging (~1 month continuous), this gel state becomes irreversible and could not be converted to sol (Figure 1).

This transformation can be accounted for the Fe^{3+} or Fe^{2+} ion-induced aggregation of negatively charged SDS micelles. Similar behavior was shown earlier by PVA–PPy dispersion. Changing the oxidant from $FeCl_3$ to ammonium peroxodisulfate (APS, which does not contain any multivalent cation), gel formation could be essentially prevented. That is the reason behind no gelling observed in PAn–SDS system studied earlier.[13] However, rate of polymerization of pyrrole by APS is too rapid to retain the stability of the dispersion for long.

Use of very large amount of pyrrole or SDS was avoided because the former might hamper the stability of the system, whereas the latter could mask the properties of PPy. Eventually, investigation was limited within only few PPy–SDS combinations, and rheological properties were explored by changing other conditions. Changing Py : SDS mole ratio (R), a set of dispersions were prepared, out of which three with $R = 0.87$ (0.2/0.23), 1.14 (0.26/0.23), and 1.43 (0.33/0.23) were selected for detailed analysis. Henceforth, these samples will be indicated as PPS-I, PPS-II, and PPS-III, respectively.

Particle Size Analysis: Transmission Electron Micrograph and DLS

Transmission electron micrograph (TEM) images [Figure 2(A–C)] taken after drying on grid cannot provide the true dynamic structure present in the solution. However, an idea on the size and morphology of PPy particles as well as micellar shape and mutual orientation of polymer and surfactant can be grown from the images left on the grid. At lower SDS concentration (0.15M), PPy particles of two different sizes are seen [Supporting Information Figure 1(A)], larger particles with diameter of 20–30 nm and smaller particles with 2–10 nm. Larger particles are essentially surrounded by the SDS shell, which is the key to the stability of the solution; smaller particles might be free polymers but owing to their smaller size they are not macroscopically precipitated out from the medium. At experimental SDS concentration (0.23M), formation of free PPy is almost prevented, and spherical PPy–SDS particles (black) visually embedded in the SDS matrix [Figure 2(A)] are observed that supports the suggested core–shell-type orientation.

It should be reminded that dilution of the dispersion for TEM and DLS was done using SDS solution of identical concentration (instead of water); therefore, we can expect no significant change in micelle structure on dilution. At higher SDS concentration [0.3M, Figure 2(B)], elongated PPy particles (~10–20 nm) are found to be surrounded by irregularly shaped SDS micelles. In some places, the composite micelles are seen to be agglomerated to form large structures. Therefore, on changing the concentration, SDS morphology of PPy particle changes from spherical to elongated, but exact size cannot be confirmed. However, considering nanoscopic dimension of the dispersed phase (PPy), the present system can be termed as nanodispersion or nanocolloid.

On standing the dispersions, Fe^{3+}-assisted physical crosslinking among the composite micelles takes place that leads to the

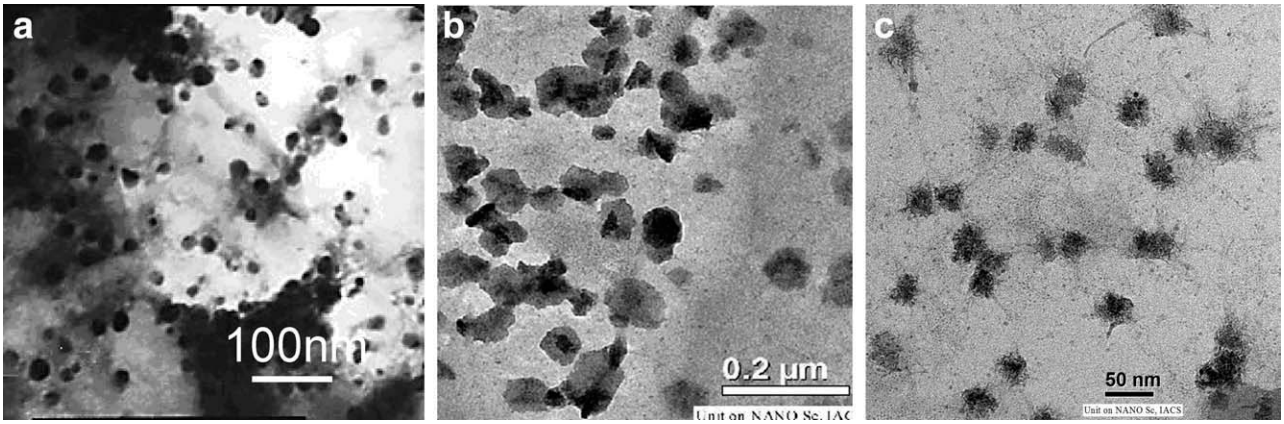

Figure 2. TEM image of PPy–SDS dispersion: (A) 0.23M SDS ($R = 1.14$), (B) 0.30M SDS ($R = 0.67$), and (C) 0.23M SDS ($R = 1.14$, after 7 days).

Applied Polymer SCIENCE

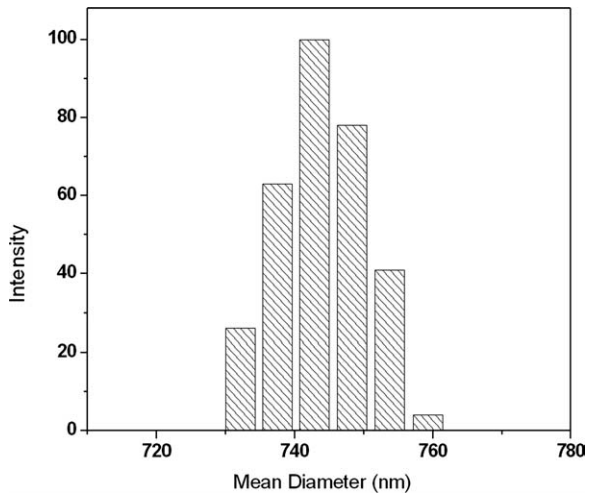

Figure 3. Representative result of DLS study showing particle size distribution in PPy–SDS dispersion ($R = 0.87$).

formation of a soft gel. At the initial stage (<10 days), the physical appearance of the dispersion is not visibly changed; however, partial crosslinking of micelles can be visualized from TEM images of diluted dispersions [Figure 2(C) and Supporting Information Figure 1(B)]. After prolonged standing, exhaustive crosslinking takes place and the gel becomes rigid. At this stage, TEM image could not be obtained. From the SEM image of PPy–SDS gel [Supporting Information Figure 1(C)], presence of large, interconnected spherical and elongated structures can be observed.

Particle size analysis of PPy–SDS nanodispersion ($R = 0.87$) using DLS technique (Figure 3) exhibits a narrow size distribution closely spaced at ~743 nm. Critical micelle concentration (CMC) of SDS is reported to be 8.0 m*M*, and the micellar diameter and aggregation number at CMC are 6 nm and 62, respectively.[16] At 0.2*M* transition, micelle structure of SDS changes from spherical to tubular form. In SDS–Fe^{3+} solution (0.23*M*), two types of particles with dimensions 9 and 34 nm are identified (not shown), which indicates either some degree of association of SDS micelles or its transition to tubular form. During polymerization of pyrrole, smaller structures are joined to form much larger ones with the PPy particles encapsulated in the SDS shell. Therefore, DLS studies in this case correlate to the dimension of PPy–SDS composite micelles, rather than free PPy particles. However, during dilution and sonication, these large aggregates are broken and, therefore, are not observed in TEM images.

UV–Vis Spectroscopy

PPy–SDS nanocolloid was diluted 20–50 times and subjected to UV–vis spectroscopic measurements, as shown in Figure 4. Similar curve was obtained from two colloids ($R = 0.87$ and 1.43), showing sharp maxima at 483 nm (2.6 eV) and broad maxima at around 890 nm (1.4 eV). These bands correspond to the transitions from valence band to bipolaron and antibipolaron bands. No peak at around 400 nm, corresponding to transition from valence band to polaron band, is observed; this indicates heavily doped nature (only bipolaron) of PPy in the dispersion.[17,18]

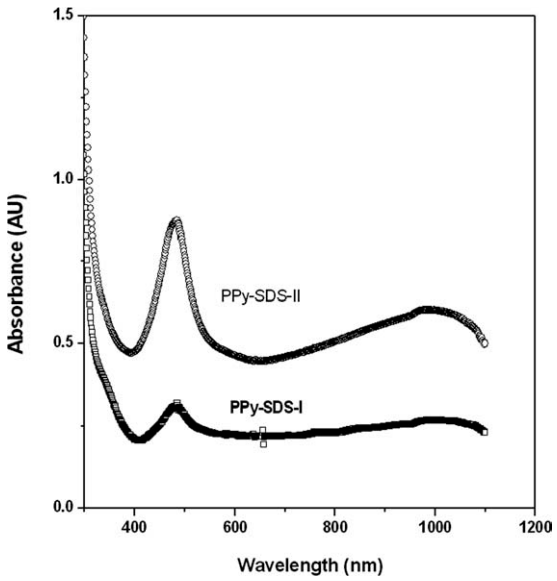

Figure 4. UV–vis spectroscopic studies on PPy–SDS dispersions.

Rheology: A. Steady

In this study, we have prepared PPy–SDS samples by changing the SDS : pyrrole molar ratio. Steady and dynamic rheological responses under different experimental conditions were monitored. Viscosity and torque of SDS solution itself having concentration identical to that used for PPy stabilization (0.2–0.3*M*) are not enough to reach the lower torque limits of instrument, and therefore a solution with much higher concentration (1.5*M*) was used for control study. The behavior of SDS solution and PPy–SDS colloids under steady shear rate sweeping is shown in Figure 5. All these systems exhibit Non-Newtonian behavior, and shear thinning is generally observed for these samples; however, for SDS solution, the thinning is almost leveled off above the shear rate 1–5 s^{-1}, whereas for PPy–SDS continuous and regular thinning is taking place throughout the

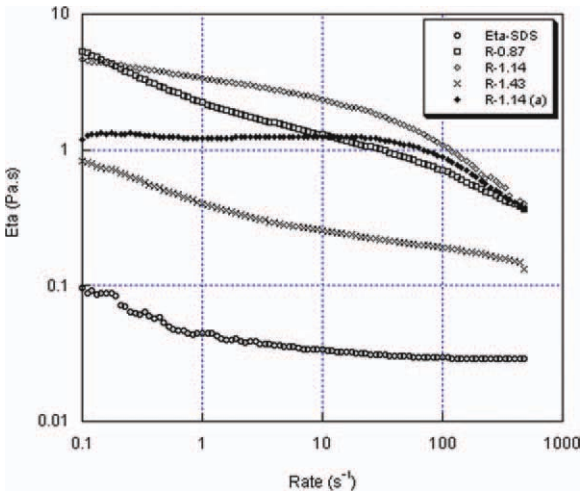

Figure 5. Results of steady shear rate sweeping on PPy–SDS nanodispersions. [Color figure can be viewed in the online issue, which is available at wileyonlinelibrary.com.]

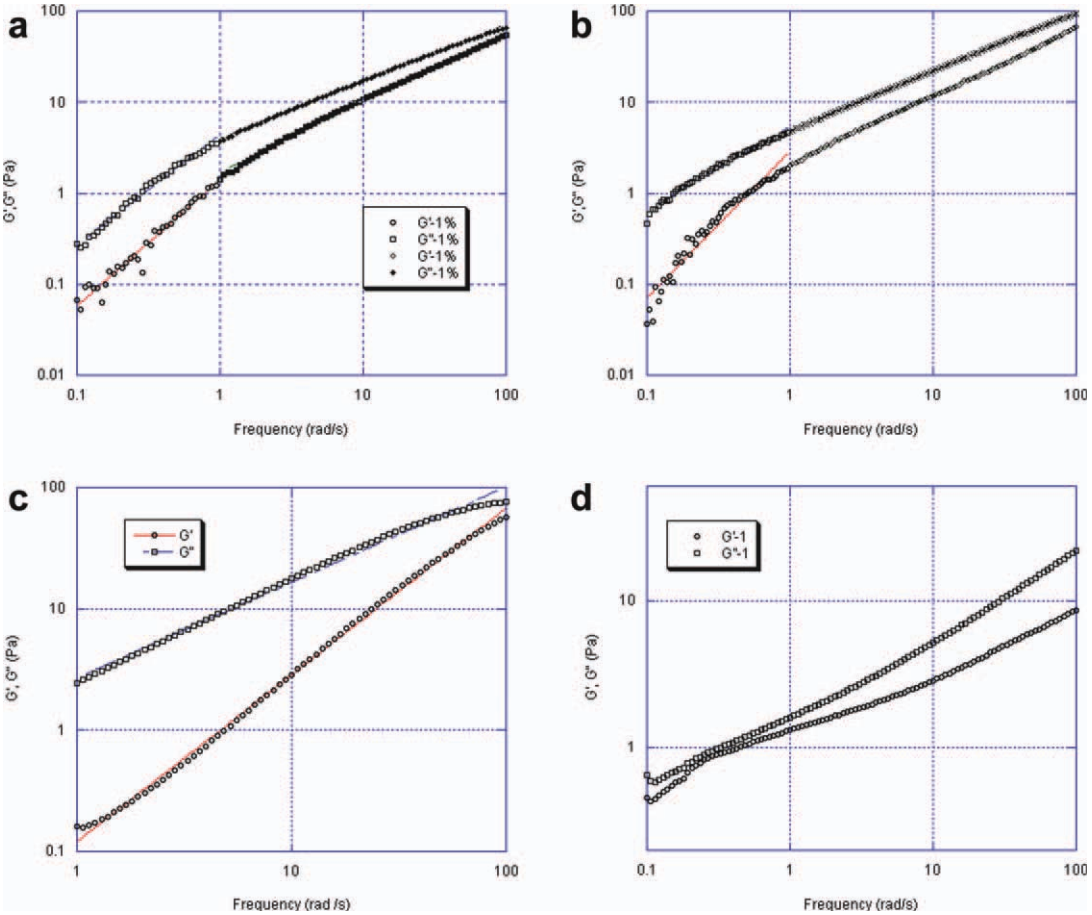

Figure 6. Frequency dependence of G' and G'' of (A) PPS-I (1%), (B) PPS-I after preshear, (C) PPS-II (1%), and (D) PPS-III (1%). [Color figure can be viewed in the online issue, which is available at wileyonlinelibrary.com.]

range (up to 500 s^{-1}). Therefore, the SDS solution itself shows Non-Newtonian behavior followed by Newtonian behavior, whereas for the PPy–SDS dispersions, Non-Newtonian behavior is observed all over the range.

After aging the dispersions for 7 days, steady viscosity profile changes and a plateau is appeared, followed by slow shear thinning at higher shear rate (>50 s^{-1}). On raising temperature, increased thermal energy hampers the interaction among the micelles, and viscosity of PPy–SDS system is gradually lowered with retention of shear thinning behavior up to 35°C (Supporting Information Figure 2). At more elevated temperature (50°C), the micelle structure is broken to large extent and some irregularity is observed. Therefore, it can be stated that the large structures formed in the PPy–SDS system are broken at higher temperature and high shear rate.

Rheology: B. Dynamic

Variation of PPy Fraction. Strain sweep experiment was carried out over a range of strain amplitudes (0.1–500%) from which linear viscoelastic (LVE) region of the PPy–SDS system was found to be within 10% (Supporting Information Figure 3). In this study, we have followed frequency-dependent variation of storage and loss moduli of PPy–SDS dispersions at different compositions, strain amplitude, and temperature. Mechanical spectrum of the system as shown in Figure 6(A–D) describes the variation of G' and G'' of PPy–SDS dispersions with three different PPy : SDS ratios (R = 0.87, 1.14, and 1.43).

Looking at the individual frequency sweep curves, different behavior of PPy–SDS dispersion was observed. For PPS-I, both G' and G'' rise sharply at lower frequency and become almost converging at higher frequency [Figure 6(A)]. On applying a preshear of 10 min at 50 $rads^{-1}$ with same amplitude, the profile of PPS-I changes. At terminal regime (<10 $rads^{-1}$) G' rises more sharply than G'' ($G'/G'' \sim 1.8$), whereas at viscous regime (>10 $rads^{-1}$) G' and G'' become almost parallel to each other [Figure 6(B)]. On increasing pyrrole concentration (R = 1.14, PPS-II), the general nature of the G' and G'' curves is affected [Figure 6(C)], and a more obvious point of convergence is approached at very high frequency. Here, the slope of G' curve is more than double to that of G'', but a real crossover does not appear within the experimental frequency range. PPS-II does not exhibit any effect of preshearing (Supporting Information Figure 4). In PPS-III, the curves converge at very low frequency and diverge thereafter [Figure 6(D)]. None of these systems, however, observe a crossover point beyond which $G' > G''$. Therefore, in the freshly prepared colloids, G' is normally lower than G'', which implies that the system behaves like a viscous liquid at this frequency range, rather than a structured liquid or gel.[19–21]

Applied Polymer SCIENCE

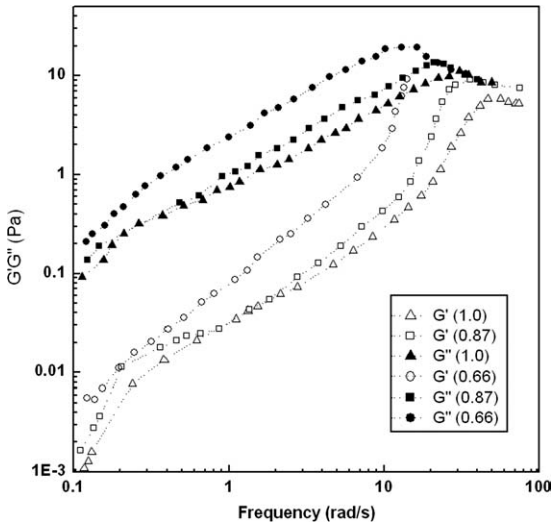

Figure 7. Frequency dependence of G' and G'' of PPy–SDS dispersions aged by 7 days with increasing SDS (numbers in bracket indicate concentration of SDS).

However, behavior of G' in this case indicates some kind of structuring present in the system, not as rigid as in a gel.

It is very interesting to note that on leaving the dispersion for 7–10 days the shear response of the dispersion at higher frequency is remarkably changed. Dynamic mechanical spectra of the aged samples varying in Py : SDS ratio are shown in Figure 7. Both G' and G'' are regularly increasing at lower frequency (terminal region); above 10 rads^{-1}, G' increases steeply and then shows a flattening trend, whereas G'' shows a clear maxima. There is a crossover point beyond which either $G' > G''$ or both curves are overlapping. Therefore, a weak gel-like behavior is observed for aged samples. By reducing Py–SDS ratio (i.e., increasing proportion of SDS), the gel-like behavior becomes more obvious, the crossover point becomes sharp and is shifted toward lower frequency. In the sample with $R = 0.66$, soon after the crossover (at ~20 rads^{-1}), the torque of the system becomes too high to continue the experiment (Supporting Information Figure 5). If the solution is left unperturbed for 15 days, it is visibly transformed to a soft gel (Figure 1)

Temperature Dependence. The effect of increasing temperature on the rheological properties of PPy–SDS dispersion has been studied, and a set of representative results (taken from the solution aged by 7 days) are shown in Figure 8(A, B). Absolute values of G' and G'' are found to be regularly lowered with increasing temperature (as observed earlier for steady viscosity); at the same time, maxima of G' and G'' are also regularly shifted to higher frequency (i.e., smaller relaxation time). By analogy with the steady viscosity, it can be interpreted as an outcome of thermally assisted breakdown of interactions among the micelles that ultimately lead to the formation of smaller structures.

Above the Krafft temperature of SDS, this effect is much more pronounced and at elevated temperature (35°C) the maximum is almost disappeared to a linear plot. Above 35°C, general behavior is lost and very irregular plot is obtained (not shown). Looking at the individual plots [Supporting Information Figure 6(A–C)], obvious overlapping/crossover of G' and G'' curves at higher frequency is observed (within 20°C). It should be mentioned that once the solution is heated up to 50°C the microstructural properties are permanently disrupted and on cooling the initial condition could not be brought back. The same experiment on freshly prepared solution also produced regular lowering of the absolute value of viscosity and moduli (figure not shown) with retention of general behavior up to 35°C.

DISCUSSION

The PPy–SDS nanodispersion studied here is a composite system, where an insoluble polymer is dispersed in a surfactant medium, a large fraction of the polymer being incorporated into the micelle as nanoparticles (not as matrix). At this point it is fundamentally different from the commonly observed polymeric solutions or the surfactant-salt systems.[22–26] Relative orientation of PPy particles with respect to the SDS micelles, which minimizes polymer–polymer interaction and leads to the

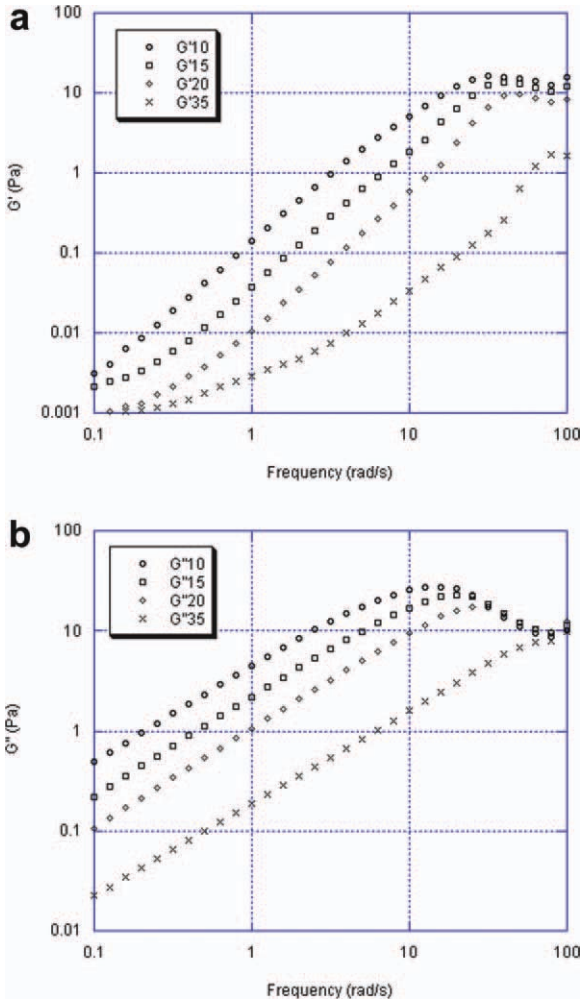

Figure 8. Classified results of frequency dependence of (A) G' and (B) G'' of PPS-II at different temperatures. [Color figure can be viewed in the online issue, which is available at wileyonlinelibrary.com.]

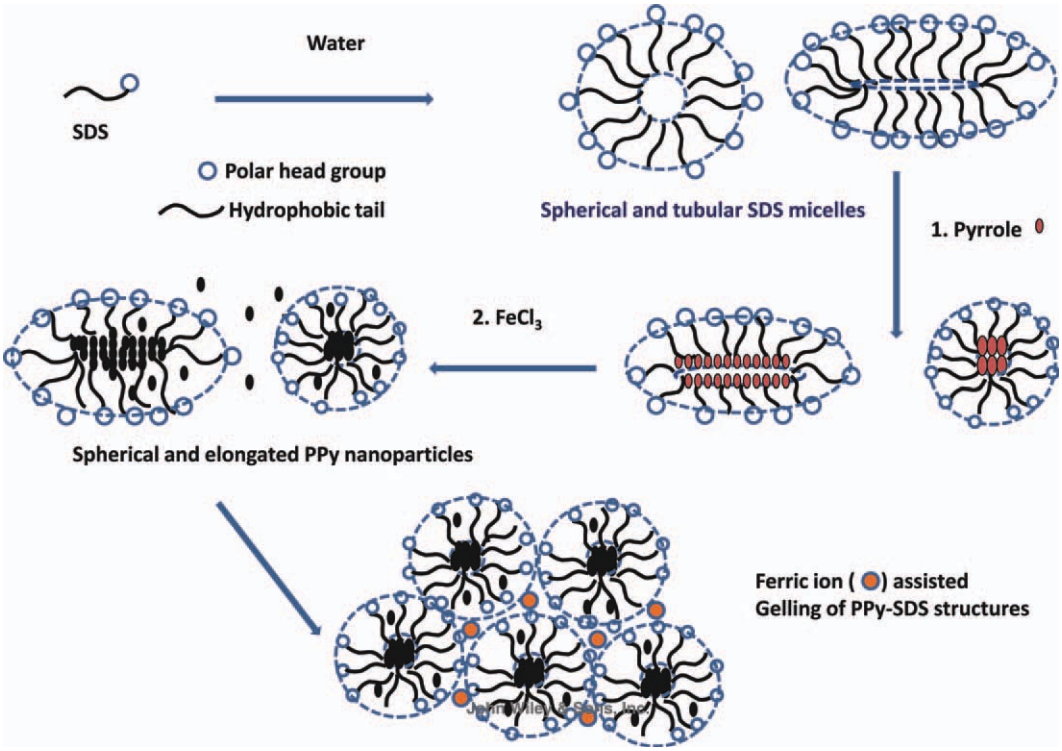

Scheme 1. Formation of PPy nanoparticles in SDS micelle. [Color figure can be viewed in the online issue, which is available at wileyonlinelibrary.com.]

formation of nanoscopic PPy particles, is a matter of fundamental interest here. Considering the hydrophobic/hydrophilic regions of the SDS micelle, PPy (hydrophobic) is supposed to be incorporated within the core. In other words, the PPy particles are surrounded by SDS micelles so that their macroscopic precipitation is prevented; that is in fact the underlying reason of the surfactant-induced stabilization of PPy. Earlier studies made by Rao et al.[9] and Kim et al.[10] on the interaction of PPy and PAn with surfactants have revealed that anionic surfactants, especially SDS, are essentially included as counteranion to the growing PPy chains during polymerization. Therefore, in this system, PPy is partially dispersed and also partially solvated by SDS micelles. Controlled particle size of PPy as well as competitive doping between Cl^- and SDS are the key to the stabilization of PPy in aqueous SDS medium. We have measured dc electrical conductivity of these dispersions using standard four-probe method from dried films on glass plates. Values of the order of $\sim 10^{-3}$–10^{-2} S cm^{-1} were obtained that is considerably lower than pure PPy powder of similar doping level. This result, however, can be accepted for the present system taking into account the incorporation of PPy within SDS shells.

It is well established that SDS shows two critical micellar concentration (CMC-I and CMC-II) values at 8 and 200 m*M*. Globular micelles in CMC-I regime and elongated/tubular/worm-like micelles in CMC-II regime are frequently observed although such dynamic structures are largely dependent on composition of the medium (surfactant : salt ratio, etc.). Beyond CMC-II bridging of micelles takes place resulting in formation of three-dimensional (3D) network-like structure.[15] Few earlier workers including Clausen et al.[27] and Watanabe et al.[28] have established that larger micelle length results in increased entanglement density and thereby higher viscosity and relaxation time of the system. These information could be correlated to the present system for explaining the rise of viscosity of PPy–SDS compared with pure SDS solution of identical concentration (0.2*M*). On addition of $FeCl_3$ to the mixture of pyrrole and SDS, pyrrole starts to polymerize, PPy particles grow bigger in size, and at the same time SDS micelles are also associated to accommodate the PPy particles (that prevent the precipitation). If the concentration of SDS is low and/or rate of polymerization is too rapid, then free PPy particles are generated at large fraction and stability of the solution is disturbed. Otherwise, all stable dispersions of this series preserve core–shell morphology of polymer micelle [TEM pictures, Figure 2(A, B)].

Therefore, it is possible that with change in concentration (0.15–0.3*M*) of SDS or Py : SDS ratio shape of SDS micelle changes from spherical to elongated/worm-like one, resulting in elongated PPy particles (Scheme I). Further association of PPy–SDS composite micelles (postpolymerization) mediated by Fe^{3+} ions gives rise to the formation of larger aggregates, arrested in DLS studies and higher viscosity of medium. Similar assemble of micelles accompanied by rise in viscosity of medium was observed earlier[13,18] where joining of micelles was mediated by aniline/pyrrole molecules.

On increasing the concentration of pyrrole with respect to SDS (i.e., by increasing the value of *R*), shear viscosity (Figure 5) of PPy–SDS is primarily increasing and then decreasing. $R = 0.87$, 1.14, and 1.43 correspond to the pyrrole–SDS ratios as 0.2 : 0.23, 0.26 : 0.23, and 0.33 : 0.23, respectively. Therefore, for

effective stabilization of PPy particles, there is a critical value of R, above which more and more free PPy are formed. It is supposed that larger fraction of free PPy (R changes from 1.14 to 1.43) obstructs the overlapping of micelles and thereby reduces the degree of entanglement of micelles. In a recent work, Park et al.[29] have published rheological data on Ag nanoparticle suspension in polyacrylic acid (PA). They have also observed similar behavior of shear viscosity with respect to PA : Ag ratios that indicated the existence of a critical value of R.

Shear thinning is a very common phenomenon in polymer systems, arising from shear-induced breakdown of internal structures and alignment of microstructures with the flow direction, reducing local drag.[30] With increase of steady shear rate, alignment with flow becomes more complete and shear viscosity is further lowered. In most of the polymer solutions, a 3D network-like structure is formed by weak physical bonds (e.g., hydrogen bonding), which is gradually disrupted on high shear resulting in shear thinning. Moreover, presence of hydrophobic associations gives rise to some degree of shear-induced structuring that prevents the thinning effect and results in a plateau. At this point, a micelle-based system such as PPy–SDS encounters a fundamental difference. In PPy–SDS, large micellar entanglements can build 3D structures, but the system does not have enough rigidity like a polymer solution to undergo any shear-induced structuring. Therefore, under shear, the 3D structure suffers continuous disentanglement and breakdown resulting in regular lowering of viscosity. From the observed change of viscosity with shear rate, it seems that PPy–SDS dispersion does not have yield stress properties. This behavior of PPS-I, II, and III is very close to that of a 0.5–2.0% cellulose solution.[31] Shear thinning under high shear (500 s^{-1}) makes PPy–SDS suitable for application as paint or ink.

After aging the dispersions by 7–10 days, PPy–SDS composite micelles are gradually agglomerated by slowly developing electrostatic interaction via Fe^{3+} ultimately leading to a gel. Therefore, the solution aged by 7 days is partially agglomerated and acquire enough rigidity compared with polymeric systems to undergo some shear-induced structuring. As a result, a broad viscosity plateau very similar to the polymeric solutions followed by a shear thinning region appears [$R = 1.14$(a)] in the rheological profile of aged sample. However, the reason of viscosity lowering of aged samples compared to the freshly prepared one ($R = 1.14$) is not very clear. After prolonged aging (>20 days), the sample is irreversibly transformed to gel.

In the filled polymer systems, internal structures are formed from the filler–filler interaction; in that case, the filler agglomerates are essentially broken under a small critical shear independent of the frequency of test.[32] In PPy–SDS system, the surfactant micelles and the polymer chains are oriented in a very complicated fashion where connections among the dispersed particles occur through the links of the matrix. That is why the disruption of the internal structure depends on both the strain (%) and frequency of the experiment. At lower frequencies, the entanglements get enough time to be broken and rebuild so that critical strain required for structural disruption is very large. At higher frequency, the network has less time to rebuild the broken links and the structural breakdown becomes obvious at lower strain amplitude. However, the critical amplitude (at onset of nonlinearity) is shifted to lower with increase of frequency that implies the existence of a weak/semirigid network structure, readily ruptured as soon as the product of amplitude and frequency exceeds a critical value. Beyond the LVE regime (i.e., above 10% strain), the effect of strain amplitude is almost minimized, especially at higher frequency, and the respective plots are superimposed (not shown).

The simplest mechanical model generally applied to mechanical properties of the surfactant systems is the Maxwell model. According to this model, a viscoelastic surfactant solution is described as a combination of a spring and a dashpot corresponding to the shear rigidity (G_N^0) and a viscosity (η) in series or in parallel.[2] The behavior of a Maxwell material under harmonic oscillation can be obtained from the following equations:

$$G'(\omega) = G_N^0 \omega^2 \tau^2/(1+\omega^2\tau^2)$$
$$G''(\omega) = G_N^0 \omega\tau/(1+\omega^2\tau^2),$$

where ω is the angular frequency in rad s^{-1} and τ is the "relaxation time" defined as time required for stress relaxation (s). G' (storage modulus) and G'' (loss modulus) correspond to the viscous component and elastic component of the solution, respectively. The respective Cole–Cole plot (plot of G'' as a function of G') of a Maxwell system fits perfectly to a semicircle.[23,27] However, to explain the behavior of systems with a range of relaxation times, Maxwell model is quite insufficient and different modifications were made later on.

Deviations from Maxwell model have been noticed earlier by different groups of investigators, and few corrections were introduced. Two other models proposed in this context by Rouse and Zimm[33,34] could explain rheological behavior of the dilute solution of a flexible, randomly coiled polymer macromolecule. Both these models consider the system as a combination of N numbers of identical beads joined together by $(N-1)$ identical Hookean springs. Despite few differences in the underlying principles, both the theories predict the low frequency slopes of 2 and 1, respectively, for G' and G'' plots for linear viscoelastic materials. In high-frequency region, the Rouse theory[33] predicts overlapping of two modulus curves with a slope of 0.5; the relevant equation is as follows:

$$[G']_R = [G'']_R = \pi(\tau_R\omega)^{1/2}/2\sqrt{2}, \quad (1)$$

where τ_R is the longest relaxation time in the Rouse spectrum.

On the other hand, Zimm theory[34] obeys the following relations:

$$[G']_R = 1.05(\tau_z\omega)^{2/3} \quad (2)$$

and

$$[G'']_R = 1.82(\tau_z\omega)^{2/3}, \quad (3)$$

where τ_z is the first Zimm relaxation time.

Therefore, according to Zimm theory,[34] two modulus curves are parallel (at higher frequency) and approach a slope of 0.67 and are separated by a factor of 1.73. Tam and Tiu[35] and Zirnsak et al.[36] have applied these models to explain the dynamic rheological behavior of four polymeric solutions namely, polyacrylamide, xanthan gum, carboxymethyl cellulose, and poly ethylene oxide (PEO).

Dynamic mechanical spectra of three PPy–SDS dispersions have revealed that freshly prepared PPy–SDS dispersion is a viscous fluid ($G''>G'$) over the whole range of frequency and amplitude. At lower frequency, sharp rise of G' and G'' corresponds to regular disentanglement and reorientation of micelles, resembling to polymer chains[37,38] and development of solution anisotropy according to the direction of the shear.[25] For PPS-I slopes, G' and G'' curves (Table I) are closer ($\infty\ \omega^{1.38}$ and $\omega^{1.21}$) and at higher frequency they are gradually leveled off to almost convergence [Figure 6(A)]. This behavior of PPS-I resembles to reversible polymer network (weak gel) characterized by closer power law dependence of G' and G'', similar to hydrophobic alkali soluble emulsion (HASE) polymers.[37] For PPS-II, on the other hand, steep rise of both G' and G'' curves followed by a point of convergence is observed [Figure 6(C)] at the highest frequency range examined (>10 rad s^{-1}). PPS-II, therefore, behaves more or less like semidilute polymer solutions following any of Rouse or Zimm model (with G'/G'': 1.7, close to theoretical value 2).

Earlier, we have seen that viscoelasticity of PVP solution satisfactorily fits Zimm model with $N = 1$.[39] Lowering in the values of slope and intercept might be accounted for the interchain interaction present in the system that was not considered in the original model (suggested for 0.1% w/v solution). Similar deviations were encountered earlier in case of PAn–PVP and PAn–SDS dispersions.[12,13] In PPS-III [Figure 6(D)], an overlapping point is found at a frequency (0.45 rad s^{-1}) close to the lowest end of the accessible frequency range. However, up to the point of convergence PPS-III (having very high PPy fraction) also maintains larger slope for G' (~1.5 times to that of G''), although frequency dependence in general is very weak ($\infty\ \omega^{0.72}$ and $\omega^{0.475}$).

Therefore, depending on the PPy : SDS ratio nature of dynamic spectrum changes and position of overlapping point also changes. However, the system never works like a full network ($G' > G''$). Absence of plateau/maxima and crossover/overlap between G' and G'' curves indicates that the relaxation process is not clearly recognized within the experimental frequency range. Rather, a spectrum of relaxation processes is suggested similar to entangled polymer solutions where different configurational motions of flexible chains are possible. Considering the complicated nature of the system, compared with a polymeric or DNA[40] solution, discussed earlier, we could not include concentration and molecular weight factors (to compare with hybrid model). Interestingly, after application of preshear for 10 min to PPS-I, mechanical spectrum is somewhat changed [Figure 6(B), Table I]. Applied preshear affects the nature of spectrum and the system approaches toward terminal behavior of a semidilute polymeric solution ($G' \sim \omega^2$ and $G'' \sim \omega$), closer to Zimm model. This is evidence in support of loosely crosslinked/weak gel-like nature of the system. On application of shear, the crosslinks are broken and the system tends toward sol-like behavior. For PPS-II, preshear leaves no effect on G' and G'' curves, which supports its semidilute solution-like nature.

Table I. Slopes of G' and G'' of Different PPy–SDS Dispersions at Terminal and Viscous Zones

Sample (temp. 25°C)	Frequency sweep slope			
	Terminal		Viscous	
	G'	G''	G'	G''
PPS-I (1%)	1.38	1.21	0.77	0.624
PPS-I (1%, preshear)	1.61	0.91	0.74	0.65
PPS-I (10%)	1.24	0.81	0.69	0.59
PPS-II	1.35	0.79		
PPS-III	0.72	0.475	-	-

Summarily, in the samples with lower PPy fraction, weak gel-like behavior becomes obvious. With an increase of PPy fraction, entanglement density is reduced and the system behaves like polymeric solution. Earlier, Ikeda and Nishinari[41] have shown that aqueous solution of κ-Carrageenan exhibits shifting of crossover point to lower frequency and a transition from dilute polymeric solution to weak gel by increasing concentration. Solution of pulp cellulose in an ionic liquid studied by Kuang et al.[31] has also exhibited similarity with PPy–SDS. The present system is fundamentally different from a single polymeric solution, and we cannot fit all the results to any of the existing models. However, it behaves more or less like a solution/dispersion and never shows a purely gel-like behavior ($G' > G''$) at freshly prepared stage.

Earlier, we have observed that hydrogen bonding can result in weak crosslinking of PVP chains, affecting rheological features of PAn–PVP system[12] on standing. Crosslinking of the present system on aging and its ultimate transformation into gel has already been discussed. Partially crosslinked samples aged by 7 days (after extensive crosslinking, rheological profile cannot be studied) were therefore selected for rheological studies. After few days of synthesis, micelles are gradually aggregated by electrostatic interaction via Fe^{3+} (not by any chemical bonding/crosslinking) and form a 3D network. Therefore, absolute values of moduli of this system are not comparable to the polymeric gels. The network, although weak, cannot relax properly at higher frequency, which causes G' to increase sharply at higher frequency and overlap with G'' immediately after the maxima. On increasing the relative concentration of SDS, moduli values increase and respective maxima of G' and G'' are regularly shifted (Figure 7) to lower frequencies, implying longer relaxation time (τ). According to Clausen et al.,[27] increase in τ and G_N^0 is an indication of growth of the tubular- or worm-like micelles in length. By analogy, it can be suggested that for the present system increase in SDS concentration results in growth of the micelles and corresponds to delayed relaxation phenomena. Increase in PPy concentration, on the other hand, disturbs the self-interaction among SDS micelles and results in relatively

Table II. Slopes and Relaxation Time Values Obtained from PPS-II at Different Temperatures

Temperature (°C) (sample: PPS-II)	Overlapping frequency (ω)	Terminal slope		Relaxation time (s) ($\tau = 1/\omega$)
		G'	G''	
10	31	1.66	0.89	0.03225
15	50	1.56	0.96	0.02
20	63	1.47	0.98	0.016

smaller structures. G' and G'' values are also lowering accordingly (Supporting Information Figure 7).

Temperature-dependent mechanical spectrum of PPy–SDS over 10–35°C [Figure 8(A, B)] matches qualitatively to that of reversible network systems, viz., PVA/borate system[29] or hydrophobically modified ethylene oxide urethane (HEUR) systems.[42] Both G' and G'' increase steeply at lower frequencies and overlap at terminal frequency regions, roughly following Maxwell model (single unit) with single relaxation time. However, there is some deviation from Maxwell behavior because the crossover point does not overlap with the maxima of G'' (Supporting Information Figure 6). Therefore, PPy–SDS system at lower temperature follows Maxwell model only up to the point of crossover.

Slopes of G' and G'' curves, overlapping frequency, and relaxation time values at different temperatures are given in Table II. With lowering temperature below 20°C, the crossover point is shifted to lower frequencies while slopes of $G' > G''$ (>1.5 times at 10°C). Therefore, with lowering temperature below the Krafft temperature of SDS (16°C) relaxation time increases, that is, the system relaxes slowly. At the same time, it is shifted from semidilute polymer-like behavior (Zimm model) to entangled polymer-like behavior (Maxwell model).

CONCLUSION

PPy–SDS nanodispersion, as stable as a solution, presents a system fundamentally different from conventional polymeric solution/dispersion/filled polymer systems. In this system, interplay of rheological properties of a surfactant and a polymer solution is observed, but polymer-like behavior is predominating. The dispersion behaves like a perfectly viscoelastic fluid (over a wide range of frequency and amplitude), and the elastic component of which comes from the weak network-like structure originating from the entanglement of micelles. Formation of large composite structures incorporating the PPy nanoparticles within SDS micelles has also been detected by the TEM and DLS measurements. However, the network is susceptible to rupture under large deformation (as revealed by the obvious strain/frequency dependence) or thermal agitation and, therefore, is not as rigid as a chemical gel. There are some special viscoelastic properties of this dispersion resembling to polymeric solutions (especially the hydrophobically modified polymers). Nature of mechanical spectra, absence of a single relaxation time, and slopes of G' and G'' curves indicate semidilute polymer solution like properties, roughly following Zimm model. PPy fraction in the dispersion ultimately controls the rheology of the system, but no regular linear relation between the initial monomer loading and viscoelastic response could be drawn. Shear viscosity of the nanodispersions is much higher than the prescribed values (0.5–40 mPa s)[43]; however, this dispersion can be diluted to any extent using SDS solution, and the viscosity can therefore be adjusted accordingly. Therefore, spherical/elongated particles, having dimension <100 nm, moderate conductivity (10^{-3}–10^{-2} S cm^{-1}), and shear thinning behavior encourage the application of freshly prepared PPy–SDS as conducting ink for sophisticate printed devices. It was further confirmed from the temperature-dependent studies that the system does not have any other special features to show (e.g., shear thickening) below Kraft temperature (16°C) of SDS (Supporting Information Figure 2). Rather, the ink/paint works well at a temperature range from 10 to 35°C.

In a parallel work,[44] we have stabilized PPy in the presence of polyvinyl alcohol and have obtained similar dependence on frequency and amplitude (Supporting Information Figure 8).

The nanodispersion remains effective as ink/paint within several days of synthesis beyond which electrostatic interaction comes into play and physical crosslinking takes part. Partially crosslinked dispersion (7–10 days after synthesis) shows a clear crossover between G' and G'' at lower temperatures (10–20°C), corresponding to at least one defined relaxation time. On standing the dispersion, electrostatic interaction becomes exhaustive and the structure becomes more rigid as reflected by the changes in appearance (transformation to soft gel) and acquired insolubility. Therefore, the coating/printed matter cannot be wiped out after drying, which favors the ink/paint application of the dispersion in some way. We have synthesized the same dispersion using APS as oxidant that does not gel on standing and might work as better ink. Rheological studies of that system will be reported elsewhere.

ACKNOWLEDGMENTS

The author is thankful to Prof. Y. Osada and Prof. J. P. Gong, Division of Biological Sciences, Graduate School of Science, Hokkaido University, Japan, for laboratory facilities and valuable suggestions. JSPS (JAPAN) and SERC-DST (INDIA) are sincerely acknowledged for financial assistance.

REFERENCES

1. Ferry, J. D. Viscoelastic Properties of Polymers, 3rd ed.; Wiley: New York, **1980.**
2. Hoffmann, H.; Rehage, H. In Rheology of Surfactant Solutions: New Methods of Investigation; Zana, R., Ed.; Marcel Dekker: New York and Basel, **1987;** p 209.
3. Gangopadhyay, R.; De, A.; Ghosh, G. *Synth. Met.* **2001,** *123*, 21.
4. Wessling, B. *Synth. Met.* **1998,** *93*, 43.
5. Gangopadhyay, R.; De, A. *Chem. Mater.* **2000,** *12*, 608.
6. Vikki, T.; Ruokolainen, J.; Ikkala, O. T.; Passiniemi, P.; Torkkeli, M.; Serimaa, R. *Macromolecules* **1997,** *30*, 4064.

7. Dhanabalan, A.; Mello, S. V.; Oliveira, O. N., Jr. *Macromolecules* **1998,** *31*, 1827.
8. Kinlen, P. J.; Liu, J.; Ding, C.; Graham, R.; Remsen, E. E. *Macromolecules* **1988,** *31*, 1735.
9. Rao, P. S.; Subrahamanya, S.; Sathyanarayana, D. N. *Synth. Met.* **2002,** *128*, 311.
10. Kim, B. J.; Oh, S. G.; Han, M. G.; Im, S. S. *Synth. Met.* **2001,** *122*, 297.
11. Garai, A.; Nandi, A. K. *J. Polym. Sci. Part B: Polym. Phys.* **2008,** *46*, 28.
12. Gangopadhyay, R. J. *Polym. Sci. Part B: Polym. Phys.* **2008,** *46*, 2443.
13. Gangopadhyay, R. J. *Colloid Interface Sci.* **2009,** *338*, 435.
14. Li L., Yang, J., Chen, X., Hao, X., *Synth. Met.*, **2009**, *159*, 2462.
15. Rehage, H.; Hoffmann, H. *Mol. Phys.* **1991,** *74*, 933.
16. van Os, N. M.; Haak, J. R.; Rupert, L. A. Physico-Chemical Properties of Selected Anionic, Cationic and Nonionic Surfactants; Elsevier: Amsterdam, **1993.**
17. Menon, V. P.; Lei, J.; Martin, C. R. *Chem. Mater.* **1996,** *8*, 2382.
18. Antony, M. J.; Jaykannan, M. J. *Phys. Chem. B.* **2007,** *111*, 12772.
19. Rehage, H.; Hoffmann, H. *Faraday Discuss. Chem. Soc.* **1983,** *76*, 363.
20. Raghavan, S. R.; Riley, M. W.; Fedliew, P. S.; Khan, S. A. *Chem. Mater.* **1998,** *10*, 244.
21. Cox, W. P.; Merz, E. H. *J. Polym. Sci.* **1958,** *28*, 619.
22. Bandyopadhyay, R.; Sood, A. K. *Langmuir* **2003,** *19*, 3121.
23. Kadoma, I. A.; Ylitalo, C.; van Egmond, J. W. *Rheol. Acta* **1997,** *36*, 1.
24. Marcovich, N. E.; Reboredo, M. M.; Kenny, J.; Aranguren, M. I. *Rheol. Acta* **2004,** *43*, 293.
25. Rehage, H.; Hoffmann, H. J. *Phys. Chem.* **1988,** *92*, 4712.
26. Raghavan, S. R.; Kaler, E. W. *Langmuir* **2001,** *17*, 300.
27. Clausen, T. M.; Vinson, P. K.; Minter, J. R.; Davis, H. T.; Talmon, Y.; Miller, W. G. *J. Phys. Chem.* **1992,** *96*, 474.
28. Watanabe, H.; Osaki, K.; Matsumoto, M.; Bossev, D. P.; McNamee, C. E.; Nakahara, M.; Yao, M.-L. *Rheol. Acta* **1998,** *37*, 470.
29. Park, B. J.; Park, B. O.; Ryu, B. H.; Choi, Y. M.; Kwon, K. S.; Choi, H. J. *J. Appl. Phys.* **2010,** *108*, 102803-1.
30. Hyun, K.; Kim, S. H.; Ahn, K. H.; Lee, S. J. *J. Non-Newtonian Fluid Mech.* **2002,** *107*, 51.
31. Kuang, Q.-L.; Zhao, J.-C.; Niu, Y.-H.; Zhang, J.; Wang, Z.-G. J. *Phys. Chem. B* **2008,** *112*, 10324.
32. Ma, S. X.; Cooper, S. L. *J. Rheol.* **2002,** *46*, 339.
33. Rouse, P. E., Jr. *J. Chem. Phys.* **1953,** *21*, 1272.
34. Zimm, B. H. *J. Chem. Phys.* **1956,** *24*, 269.
35. Tam, K. C.; Tiu, C. J. *Rheol.* **1989,** *33*, 257.
36. Zirnsak, M. A.; Boger, D. V.; Tirtaatmadja, V. J. *Rheol.* **1999,** *43*, 627.
37. English, R. J.; Gulati, H. S.; Jenkins, R. D.; Khan, S. A. *J. Rheol.* **1997,** *41*, 427.
38. English, R. J.; Raghavan, S. R.; Jenkins, R. D.; Khan, S. A. *J. Rheol.* **1999,** *43*, 75.
39. Hodgson, D. F.; Amis, E. J. *J. Chem. Phys.* **1991,** *94*, 4581.
40. Bandyopadhyay, R.; Sood, A. K. *Pramana—J. Phys.* **2002,** *58*, 685.
41. Ikeda, S.; Nishinari, K. J. *Agric. Food Chem.* **2001,** *49*, 4436.
42. Annable, T.; Buscall, R.; Ettelatie, R.; Whittlestone, D. J. *Rheol.* **1993,** *37*, 695.
43. de Gans, B.-J.; Schubert, U. S. *Macromol. Rapid Commun.* **2003,** *24*, 659.
44. Gangopadhyay, R.; Molla, M. R. *J. Polym. Sci. Part B: Polym. Phys.* **2011,** *49*, 792.